Probing Experiments on Pressure Oscillations in Two Phase and Supercritical Hydrogen with Forced Convection Heat Transfer*

by

R. S. Thurston

Los Alamos Scientific Laboratory, University of California
Los Alamos, New Mexico

ABSTRACT

Pressure oscillations induced by forced convection heat transfer to liquid hydrogen have been probed using a test section which cooled from ambient to liquid hydrogen temperatures during the course of a run. Acoustic modes due to Helmholtz and open-open pipe resonances were observed at sub and supercritical pressures. These modes did not develop when the inlet hydrogen was superheated. Pressure fluctuations in the form of sawteeth, negative pulses, and beats were also observed above and below the critical pressure. A mode which primarily occurred above the critical pressure was observed. One associated with subcritical two phase flow was also observed. Experimental evidence indicated that heat transfer at low flow rates was substantially better in two phase flow than in supercritical flow, that at moderate flow rates the pressure drop increased after the outlet hydrogen temperature leveled off at a minimum, and that larger axial wall temperature gradients were obtained in slow cooldowns than in fast ones.

---

* Work performed under the auspices of the U. S. Atomic Energy Commission

DISCLAIMER

Definitions

In this paper supercritical will mean above the critical pressure, but in the vicinity of the critical temperature.

Superheated will mean at a temperature above the saturated vapor temperature at subcritical pressures, or above the temperature at which the specific heat is maximized at supercritical pressures.

The dense state will mean a state with a temperature lower than the saturated liquid temperature at subcritical pressures, or lower than the temperature at which specific heat is maximized at supercritical pressures.

Pipe resonance will mean the resonance associated with the fundamental wavelength for an open-open pipe. For a pipe of length L, filled with a fluid at uniform temperature, this resonant frequency is given by

$$w_p = \frac{c}{2L} \tag{1}$$

Helmholtz resonance is that associated with a resonator composed of a cavity connected to an external atmosphere via an orifice or neck. The gas in the cavity is compressed and expanded by the motion of the fluid in the neck, analogous to a spring mass system. The frequency of a Helmholtz resonator consisting of a neck, containing a mass m of fluid, attached to a cavity, with volume V_G, is given by

$$w_H = \frac{A}{2\mathcal{l}}\sqrt{\frac{\gamma P}{mV_G}} \quad (2)$$

Introduction

Although heat transfer has been known for over 100 years to be capable of inducing acoustic phenomena [1]*, this investigation was chosen as a result of some relatively recent observations made in what were basically heat transfer experiments. In studies of heat transfer to gaseous hydrogen and helium, McCarthy and Wolf [2] observed that the appearance of pressure oscillations in their apparatus caused heat transfer to become independent of Reynolds number. Hines and Wolf [3] reported the destruction of thin walled test sections as a result of severe pressure oscillations accompanying heat transfer to supercritical hydrocarbons. Goldman [4, 5] has observed the production of acoustic noise, which he described as "heat transfer with a whistle" in forced convection heat transfer to two-phase and supercritical water. He has attributed this to large property variations under nonequilibrium conditions. In view of this background, probing experiments were undertaken with hydrogen at sub and supercritical pressures to establish the identity of such oscillations and to obtain some notion of the conditions under which they occur. Incidental to this investigation were general observations of cryogenic cooldown phenomena.

---

* Numbers in brackets refer to similarly numbered references in bibliography.

Apparatus

The horizontal test section, shown in Figure 1, was a 2-3/4" duraluminum rod with four holes of 3/16" diameter drilled through on a 1-1/2" circle. In some experiments three of the four holes were plugged for single channel flow studies. A vacuum jacket surrounded all upstream elements to the last 2-1/2" of a 12" inlet plenum. The remainder of the test section was blanketed with about six inches of fiberglass and several wrappings of aluminum coated mylar. Data were recorded during a cooldown from ambient to liquid hydrogen temperatures. A run was initiated with the rupture of a frangible diaphragm at the upstream end of the inlet plenum. A bleed line was installed in the inlet plenum for quick chilling of that section. A section of the vacuum jacket was in contact with the inlet plenum walls, providing a heat leak into the plenum. The outlet plenum could have either of two volumes depending on whether a volume filling plug was used. At the downstream end of the outlet plenum a metering orifice plate usually restricted the discharge flow to sonic velocities.

Static pressures were measured in both plena and one flow channel by transducers attached directly to the test section. Differential pressure between inlet and outlet plena was measured directly. Hydrogen temperatures were measured in both plena by platinum resistance sensors.

The outputs of the above instruments were continuously recorded by a high speed system in which the response was limited by the amplifiers that were used. The responses of the amplifiers were flat to the following frequencies: 250 cps for static pressures, 25 cps for differential pressure, 25 cps for temperature sensors. Wall temperatures were measured by copper-constantan thermocouples, located about 1/16 inch from the flow channels. Their outputs were sampled 20 times per second and recorded on magnetic tape. Flow rate was measured by a turbine flow meter and recorded continuously on a strip chart. Dewar pressurization and flow control loops were usually left open during the course of a run. No wall temperature asymmetry was observed between flow channels in the four channel runs. Additional details of the apparatus, operating procedures, and all experimental results are presented in an unclassified Los Alamos report [6].

Helmholtz and Pipe Resonance

Tracings from recordings of pressure oscillations are presented to illustrate the modes and fluctuations which are discussed here.

Since the test sections were proof tested with liquid nitrogen, some data were obtained using that fluid. These results illustrate phenomena occurring at frequencies much lower than those observed with hydrogen.

Figure 2 presents an observation of pipe resonance in nitrogen, illustrating the characteristic large amplitude in the flow channel and diminished amplitudes in the plena. Recorded only on nitrogen runs is the appearance of a higher harmonic in the structure of the pipe resonant mode.

Figure 3 shows Helmholtz resonance as it appeared in two experiments with similar conditions but with different outlet plenum volumes. The frequency observed with an 8.15 in^3 outlet plenum was 5.0 cps, while that observed with 27.9 in^3 was about 2.8 cps. The observed ratio of frequencies is 1.78, which differs by less than 4% from the ratio of 1.85 predicted by the formula for the Helmholtz mode. Even this small discrepancy can be accounted for if one considers that gas in the flow channels also exhibits compressibility and therefore contributes a spring effect. Furthermore, in contrast to pipe resonance, all pressure transducers recorded the same amplitude.

Figure 4 illustrates a superposition of pipe and Helmholtz resonance for hydrogen in the flow channel, a sudden cessation of the Helmholtz mode at 312.2 seconds, and a temperature-pressure phase relationship of the Helmholtz mode, noted at time 312 seconds. The sudden cessation hints at the existance of a threshold for Helmholtz resonance. The almost 180° phase difference between temperature and pressure is what one would anticipate from a pulsating flow, with heat transfer independent of Reynolds number, as McCarthy and Wolf [2] observed. In such a case, a pressure maximum is associated with a flow maximum and consequently an outlet temperature minimum.

Results from a cooldown performed at subcritical pressures in the vicinity of 150 psia are shown in Figures 5 and 6. The peak-to-peak amplitude of pipe resonance is around 3 psi and that of Helmholtz resonance below 7 psi. Although these amplitudes varied considerably from run to run, with the highest observed being 20 psi for Helmholtz and 10 psi for pipe resonance, they usually followed a pattern of building toward a peak value, and then decaying toward zero. The frequencies, as shown in Figure 6, steadily decrease as the test section cools.

Numerical calculations of hydrogen states in the test section were performed for several instances during the run, using observed wall temperatures and flow rates, and assuming the inlet fluid to be a saturated liquid. The method used [7] has only been found to be reliable for hydrogen flowing at moderate rates in long small-diameter flow channels. The calculated outlet temperatures and pressure drops appear on Figure 5. From the computed profile of hydrogen states, a pipe resonance frequency was calculated from

$$w_p = \frac{1}{2\sum\left(\frac{\Delta L}{c}\right)} \qquad (3)$$

and a Helmholtz frequency was calculated from

$$w_H = \frac{1}{2\pi}\sqrt{\frac{\gamma g P A}{(\Sigma \rho \Delta L)\ V_G}}^{1} \qquad (4)$$

These results are shown on Figure 6 and provide another means of identifying the resonant modes.

Experiments performed with three of the four flow channels plugged also showed Helmholtz and pipe resonances. In one single-channel experiment, conditions similar to those at time 295 seconds in Figure 5 occurred. The resulting Helmholtz frequency was 4.5 cps, demonstrating the flow area dependence in equation (4).

The sawtooth and pulse phenomena shown in Figures 5 and 6 will be discussed later.

Figure 7 presents the results from a cooldown conducted mainly at supercritical pressures, demonstrating the existence of Helmholtz and pipe resonance in the supercritical region. The supercritical mode, which also appears on Figure 7 will be discussed later.

Pressure Drop Phenomenon

An interesting observation, shown on Figure 7, is the rise in pressure difference occurring, after 312 seconds, with outlet temperature near a constant minimum. A comparison of measured data for times 311 and 324 is given in Table 1.

Table 1

Parameter	311 Seconds	324 Seconds
inlet pressure, psia	133	133
outlet temperature, °R	55	55
flow rate, GPM	9.2	9.1
pressure drop, psi	2.6	13.2
4" wall temperature, °R	55*	55*
13" wall temperature, °R	80	55*
26" wall temperature, °R	90	55*
39" wall temperature, °R	100	55*
Helmholtz frequency, cps	29	18

* Mean values from a recorded scatter between 50 and 60°R

The two cases present pressure drops differing by a factor of 5 for comparable inlet pressures and flow rates. The difference in Helmholtz frequency indicates a greater mass of hydrogen in the flow channels at the later time. This implies that at the later time the average quality is lower. Calculations based upon the Lockhart-Martinelli model as applied to hydrogen by Rogers [8] anticipate frictional losses to increase to a maximum with decreasing quality. However, the larger pressure drop may also be caused by a change from film to nucleate boiling, since hydrodynamic drag has been observed to be lowered by film boiling [9]. Backing this contention is the observation that all recorded temperatures in the duraluminum rod were about 55°R at the later time. In another experiment with supercritical pressures, between 200 and 250 psia, this same phenomenon was observed.

High Flow Rates and Plug Flow Oscillations

An experiment conducted with a large orifice and at relatively high flow rates also produced Helmholtz and pipe resonance, as shown in Figure 8. However, near the end of the run, at subcritical pressures, and after outlet temperature approached a stable minimum, a new pressure oscillation appeared with an amplitude in the inlet plenum larger than that in the flow channel. Other characteristics of this oscillation, illustrated in the bottom half of Figure 9, show an odd pressure drop record which is generally 180° out of phase with flow channel and inlet plenum pressures, a smooth flow channel oscillation, and a ragged inlet plenum oscillation. Under comparable conditions in a single channel experiment, this type of oscillation again appeared, but with a smooth inlet plenum oscillation, as shown in the top half of Figure 9.

Plug flow is suggested as the cause of these oscillations because a comparison of the ragged inlet plenum oscillation in four channel flow with the smooth oscillation in single channel flow suggests that a nonsynchoronous activity, such as the formation of vapor plugs, is taking place in the four channels. One can also visualize that the formation of a vapor plug would tend to back up fluid, thereby raising inlet pressure, and at the same time reduce flow rate and therefore pressure drop. Another argument for plug flow is that in the CISE experiments [10], plug flow followed a dispersed flow pattern when liquid rates were held constant and gas rates were reduced. Since hydrogen has a low surface tension it tends to disperse very easily, and only at high flow rates with the low vapor generation provided by a cold apparatus would plug flow be anticipated in this test section.

Comparing Figures 7 and 8, one notes that an increase in pressure drop did not occur after outlet temperature approached a minimum level in the high flow experiment.

Low Flow Rates and Supercritical Oscillations

Results from a very low flow experiment, in which pressure drop was almost zero, also provided something new, as shown in Figures 10 and 11. First no pipe resonance appeared, indicating that higher flow rates were necessary to excite this mode. Secondly, an oscillation appeared just as pressure ascended past the critical value. The oscillation was present while the pressure remained supercritical and disappeared as the pressure descended past the critical value. Because of its restriction to supercritical pressures, this oscillation is called the supercritical mode. Unlike the usual behavior of the Helmholtz and pipe resonance modes, the frequency of this supercritical oscillation remained nearly constant during the cooldown, as seen in Figure 11.

The third new observation made in this experiment was a rise in outlet temperature during the cooldown, when pressure fell below the critical value at 788 seconds. From this one can infer that the intensity of turbulence was greater with two phase flow than with supercritical flow.

In comparing wall temperatures for slow and fast cooldowns, much larger axial gradients were observed in slow cooldowns. For example, the run shown in Figure 8 had axial wall temperature gradients on the order of 1°R per inch, while the run shown in Figure 10 had gradients of 5.5°R per inch.

Sawtooth and Negative Pulse Fluctuations

Figure 12 illustrates sawtooth fluctuations and negative pressure pulses which were typically observed in the early phases of an experiment. These fluctuations were of equal magnitude in flow channels and plena. In the experiments performed at supercritical pressures, negative pulses were observed to accompany a rise and fall of inlet plenum temperature, as shown in the bottom half of Figure 13. When the amplitude of temperature rise lessened, the pulses degenerated into beats, as shown in the top half of Figure 13. The association of the negative pulses with a rise in inlet temperature and their amplitude dependence on the magnitude of that rise indicate this phenomenon is caused by a heat flux into the inlet plenum. One can visualize a build up of a vapor pocket by this heat flux, the dragging of the vapor into the flow stream, and finally its cooling and collasping producing a sudden decrease in pressure.

The sawtooth fluctuation and negative pulses also produced full scale fluctuations in recorded flow rates.

The low frequency oscillations shown in Figure 13 are the supercritical mode discussed in the previous section.

Dependence on Inlet Conditions

The elimination of pressure oscillations when a noticeable rise in inlet temperature occurred resulted in an investigation of inlet conditions as a requirement for pressure oscillations. A plot distinguishing oscillatory and nonoscillatory phenomena for pipe, Helmholtz, and supercritical modes on coordinates of inlet pressure versus inlet temperature is shown on Figure 14. A distinct segregation of oscillatory and nonoscillatory conditions takes place along the vapor pressure line at subcritical pressures and the locus of specific heat maxima at supercritical pressures. The latter curve appears to have the interesting property of being continuous in magnitude and slope with the vapor pressure line at the critical point. This property should not be surprising if one views the locus of specific heat maxima as the locus of states in which a maximum change in enthalpy is achieved for a small variation in temperature. Then the vapor pressure line becomes the logical extension of that locus at subcritical pressures.

The pipe, Helmholtz, and supercritical modes were generated when a dense state was present in the test section and outlet conditions were superheated. Since these oscillations did not occur in the test section when the entire flow channel was superheated, one can deduce that the mechanism for driving them occurred only in that part of the flow channel where the dense state was present.

The crossing of a temperature at which the specific heat is maximized was also observed to accompany pressure oscillations in the experiments of Hines and Wolf [3]. That this crossing is a sufficient but not a necessary requirement for pressure oscillations is seen from their appearance in the high heat flux experiments of McCarthy and Wolf [2] on all gaseous systems of hydrogen and helium. The crossing of the vapor pressure curve or the locus of specific heat maxima probably just supplies the necessary property variations under nonequilibrium conditions which Goldmann suggests as the driving mechanism of these oscillations.

Summary

In probing for pressure oscillations in two phase and supercritical hydrogen with forced convection heat transfer, five classes of pressure fluctuations were recognized:

a. Open-open pipe resonance, observed at sub and supercritical pressures, but not at very low flow rates, and identified by its predictable frequency, and confinement to flow channels;

b. Helmholtz resonance, the acoustic analogy of a spring-mass system, observed at sub and supercritical pressures, and identified by its predictable frequency, and dependence on flow area and outlet plenum volume;

c. Supercritical oscillations, appearing above the critical pressure, and usually at low flow rates;

d. Plug flow oscillations, appearing at subcritical pressures and high flow rates, and characterized by larger amplitudes in the inlet plenum than in the flow channels;

e. Sawtooth and negative pulse fluctuations, which appeared in the early phases of an experiment and were attributed to a heat flux from upstream elements.

These oscillations were observed in single and four parallel channel flow, although no asymmetry in wall temperatures surrounding different flow channels was observed in the latter case.

The presence of a dense state in the flow channels with a superheated outlet state was shown to be a sufficient condition for the generation of the pipe, Helmholtz, and supercritical oscillations.

Since Helmholtz and pipe resonance frequencies were observed to vary continuously during an experiment, the excitation of these modes probably occurs over a spectrum of frequencies.

An increase of pressure difference between inlet and outlet plena was observed at moderate flow rates after outlet plenum temperatures leveled off at a minimum. This occurred at sub- and supercritical pressures, but not at high flow rates when a plug flow pattern was believed to exist.

A rise in outlet plenum temperature was observed during a low-flow-rate cooldown as pressure went from super to subcritical, indicating an improvement in heat transfer at subcritical pressures.

Larger axial wall temperature gradients were observed in slow cooldowns than in fast ones in the duraluminum test section.

Nomenclature

A = cross-sectional flow area, in^2

C = velocity of sound, in/sec

g = gravitational constant, 386 in/sec^2

L = length, in

ΔL = increment of length used in calculations, in

m = mass of fluid in neck of resonator, slugs/12

P = pressure, psia

V_G = volume of gas in resonator cavity, in^3

V_G^1 = volume of gas in outlet plenum and flow channels, in^3

γ = ratio of specific heats

ρ = weight density of hydrogen, lbs/in^3

w_H = frequency of Helmholtz resonator, cps

w_p = fundamental frequency of open-open pipe resonance, cps

Acknowledgments

This work has been undertaken as part of a doctoral dissertation for the University of New Mexico. Chairman of the dissertation committee is Professor V. J. Skoglund; additional campus members are Professors M. W. Wildin and G. A. Whan; and the Los Alamos advisors are Drs. J. D. Rogers and W. L. Sibbitt. I am particularly grateful to the cryogenics group, CMF-9, of the Los Alamos Scientific Laboratory for the instruction and assistance they provided in the use of their cryogenic facilities.

Bibliography

1. Baron Rayleigh, The Theory of Sound, II, pg. 224, Dover Publications, New York, (1945).

2. McCarthy, J. R., and Wolf, H., "The Heat Transfer Characteristics of Gaseous Hydrogen and Helium", Rocketdyne Research Report RR-60-12, (December 1960).

3. Hines, W. S., and Wolf, H., "Pressure Oscillations Associated with Heat Transfer to Hydrocarbon Fluids at Supercritical Pressures and Temperatures", A.R.S. Jour., 32, Issue 3, pp. 361 - 366, (March 1962).

4. Goldmann, K., "Boiling Songs", NDS 10-68, (May 1953).

5. Goldmann, K., "Heat Transfer to Supercritical Water at 5000 psi, Flowing at High Mass Flow Rates through Round Tubes", Int.Devl. in Heat Transfer, ASME, pp. 561 - 568, (1961).

6. Thurston, R. S., "Pressure Oscillations Induced by Forced Convection Heat Transfer to Two Phase and Supercritical Hydrogen, Preliminary Experiments", (to be assigned a LAMS number when available), L.A.S.L., Los Alamos, N. M., (1964).

7. Thurston, R. S., and Pollock, R., "Startup Studies of a Nuclear Rocket Reactor, Part 1, Computational Procedures and Experimental Checks", Proceedings of Nuclear Propulsion Conference, TID-7653, Pt. 1, (1962).

8. Rogers, J. D., "Two Phase p-H_2 Friction Factors", Advances in Cryogenic Engineering, 8, K. D. Timmerhaus (ed), Plenum Press, New York (1964).

9. Bradfield, W. S., Barkdoll, R. O., and Byrne, J. T., "Some Effects of Boiling on Hydrodynamic Drag", Int. J. Heat and Mass Transfer, 5, pp. 615 - 622, (1962).

10. "A Research Program in Two Phase Flow", CISE (Centro Informazioni Studi Esperienze), Milan, Italy, M. Silvestri, Dir., (Jan. 1963).

Captions

Figure 1: Test Section Details.

Figure 2: Pipe Resonance in Nitrogen.

Figure 3: Helmholtz Resonance in Nitrogen.

Figure 4: Superposition of Pipe and Helmholtz Resonance in Hydrogen. Note sudden cessation of Helmholtz oscillation and phase difference between temperature and pressure.

Figure 5: Amplitudes of Pressure Oscillations During a Liquid Hydrogen Cooldown at Subcritical Pressures.

Figure 6: Frequencies of Pressure Oscillations.

Figure 7: Results from a Cooldown at Supercritical Pressures.

Figure 8: Results from a Cooldown at High Flow Rates.

Figure 9: Plug Flow Oscillations at High Flow Rates.

Figure 10: Results from a Cooldown at Low Flow Rates.

Figure 11: Frequencies of Pressure Oscillations at Low Flow Rates.

Figure 12: Sawtooth Fluctuations and Negative Pressure Pulses.

Figure 13: Negative Pressure Pulses and Beats Accompanying a Rise in Inlet Plenum Temperature at Supercritical Pressures.

Figure 14: Dependence of Pipe, Helmholtz, and Supercritical Oscillations on Inlet Conditions.

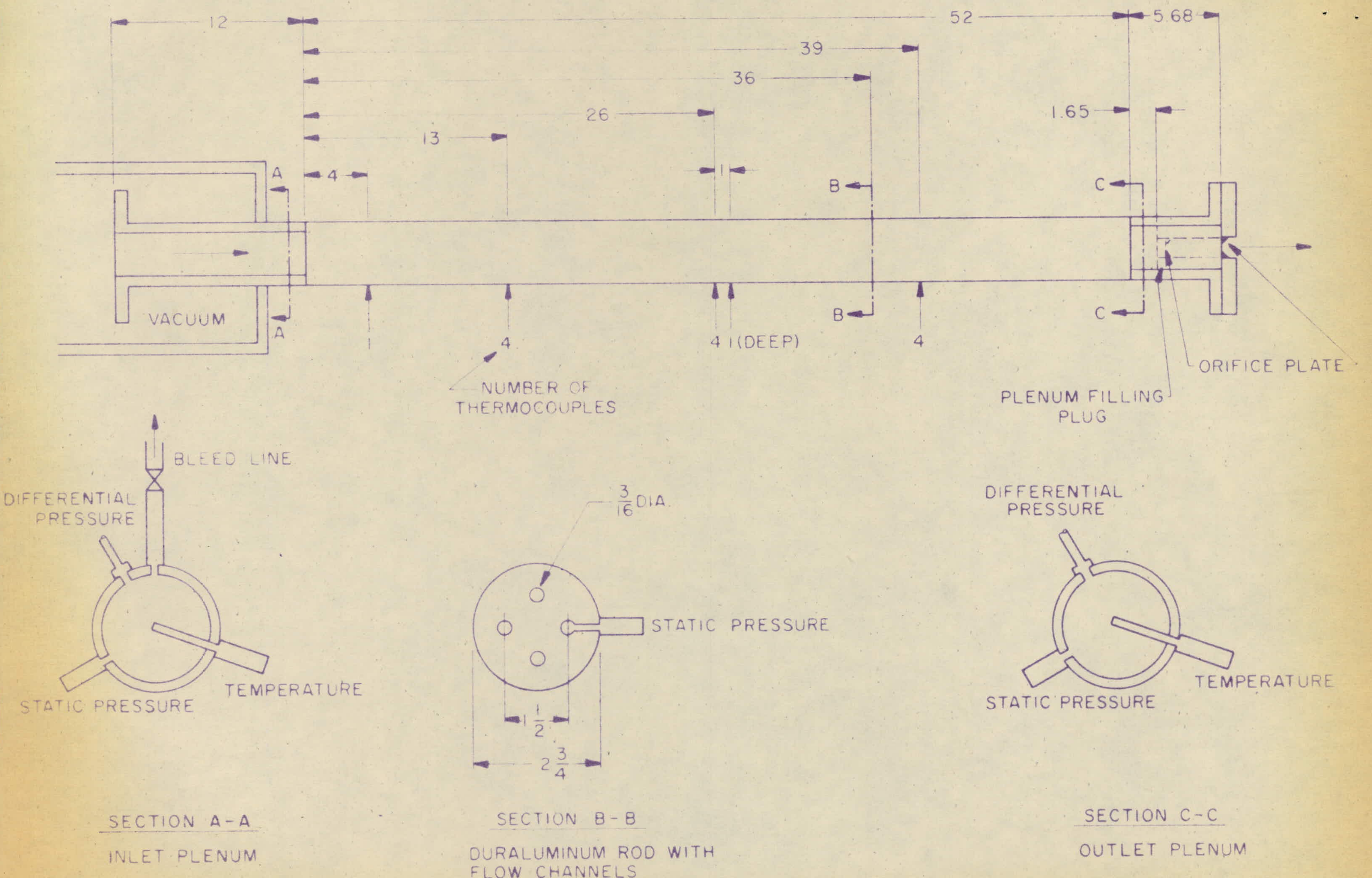
12
52
5.68
39
36
26
13
4
1
1.65
A
B
C
VACUUM
4
4
4 1 (DEEP)
4
NUMBER OF THERMOCOUPLES
ORIFICE PLATE
PLENUM FILLING PLUG
BLEED LINE
DIFFERENTIAL PRESSURE
STATIC PRESSURE
TEMPERATURE
SECTION A-A
INLET PLENUM
3/16 DIA.
STATIC PRESSURE
1 1/2
2 3/4
SECTION B-B
DURALUMINUM ROD WITH FLOW CHANNELS
DIFFERENTIAL PRESSURE
TEMPERATURE
STATIC PRESSURE
SECTION C-C
OUTLET PLENUM

FIGURE 1

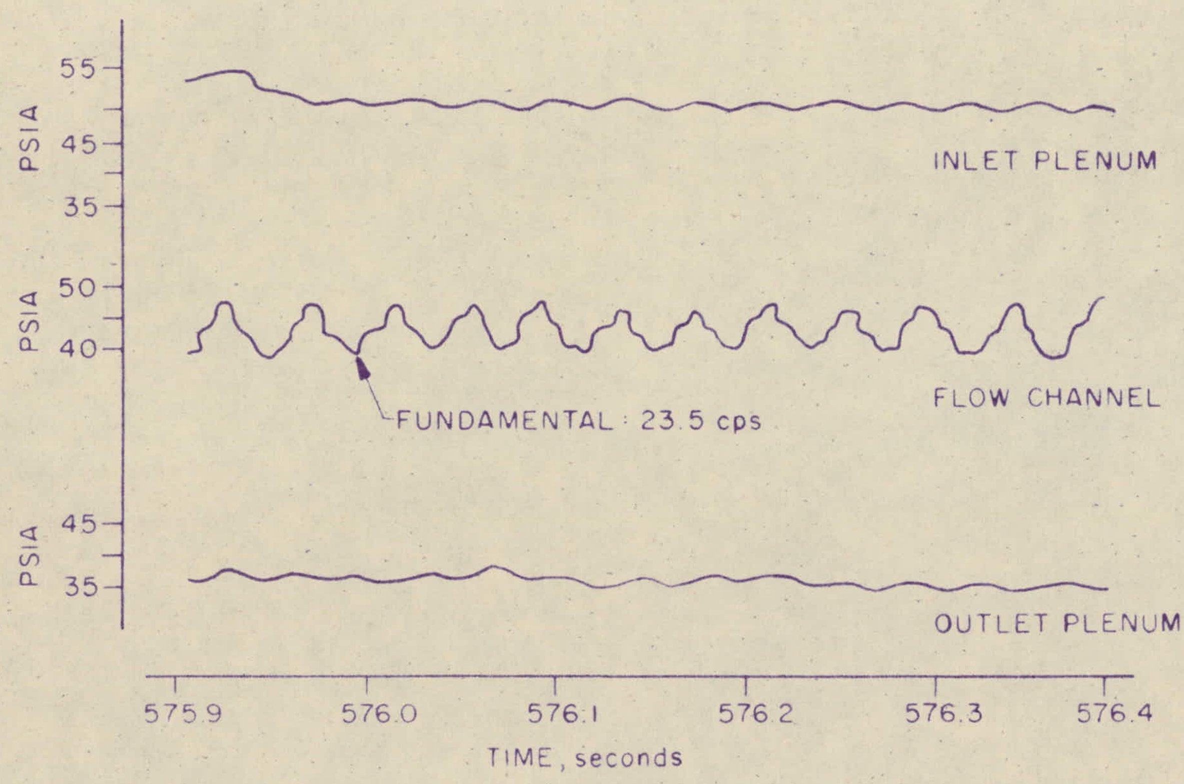

NITROGEN EXPERIMENT OF SEPTEMBER 30, 1963
130 °R AT INLET, 160 °R AT OUTLET
8.15 in.^{3} OUTLET PLENUM, 0.203 in. ORIFICE

FIGURE 2

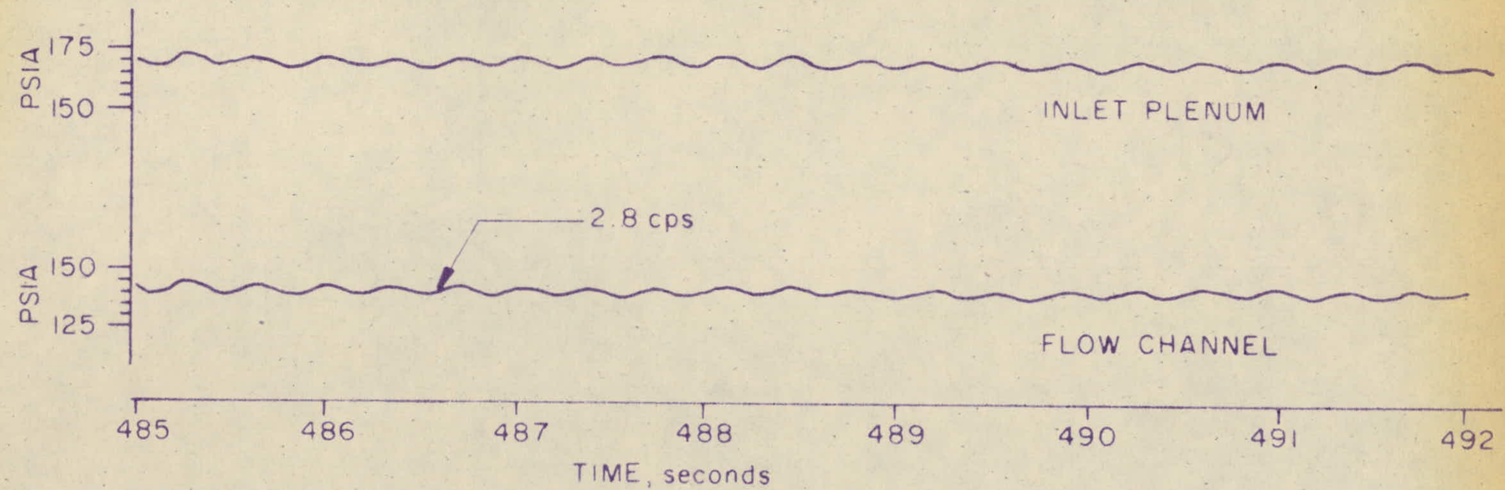

NITROGEN EXPERIMENT OF OCTOBER 2, 1963
INLET TEMP. SENSOR INOPERATIVE, 200 °R AT OUTLET
27.9 in^3 OUTLET PLENUM, 0.07 in. ORIFICE

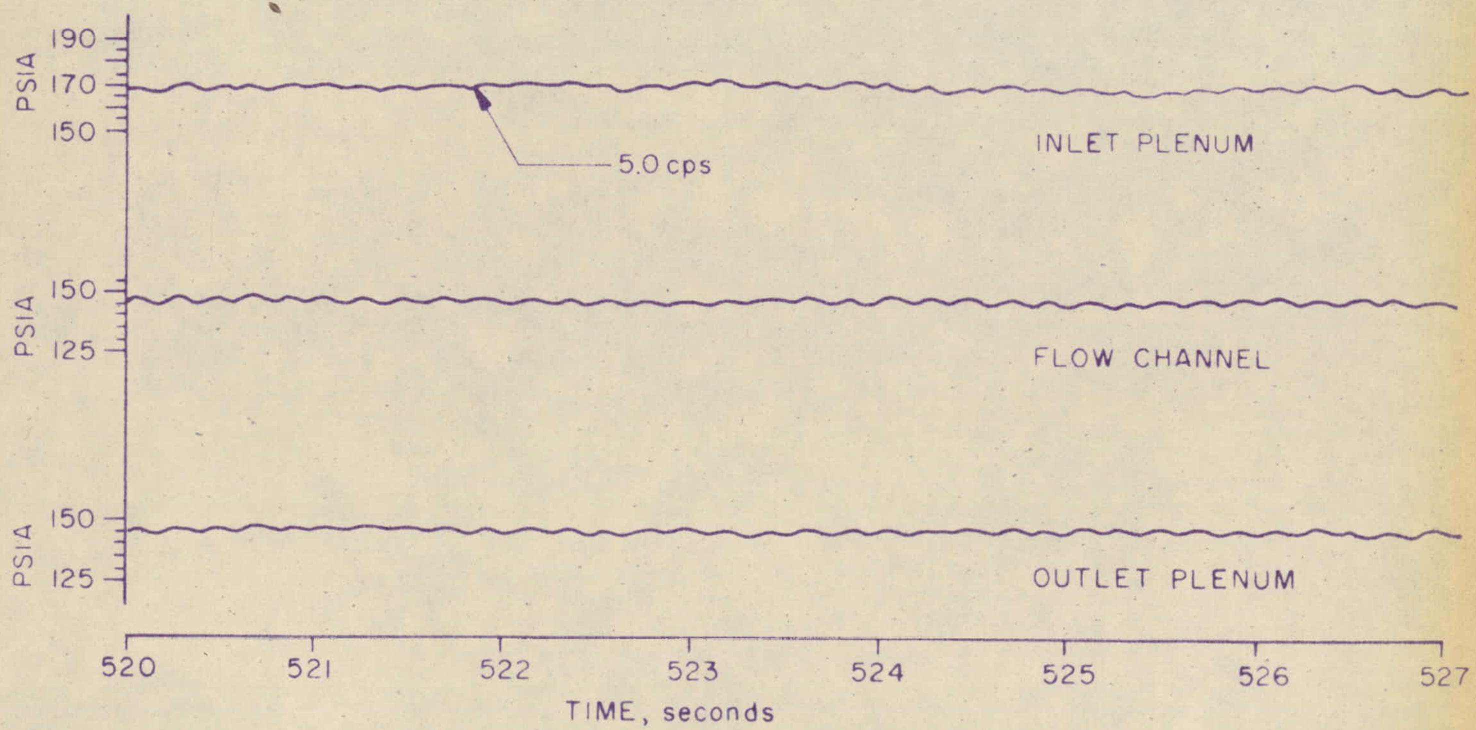

NITROGEN EXPERIMENT OF OCTOBER 1, 1963
158 °R AT INLET, 200 °R AT OUTLET
8.15 in^3 OUTLET PLENUM, 0.07 in. ORIFICE

FIGURE 3

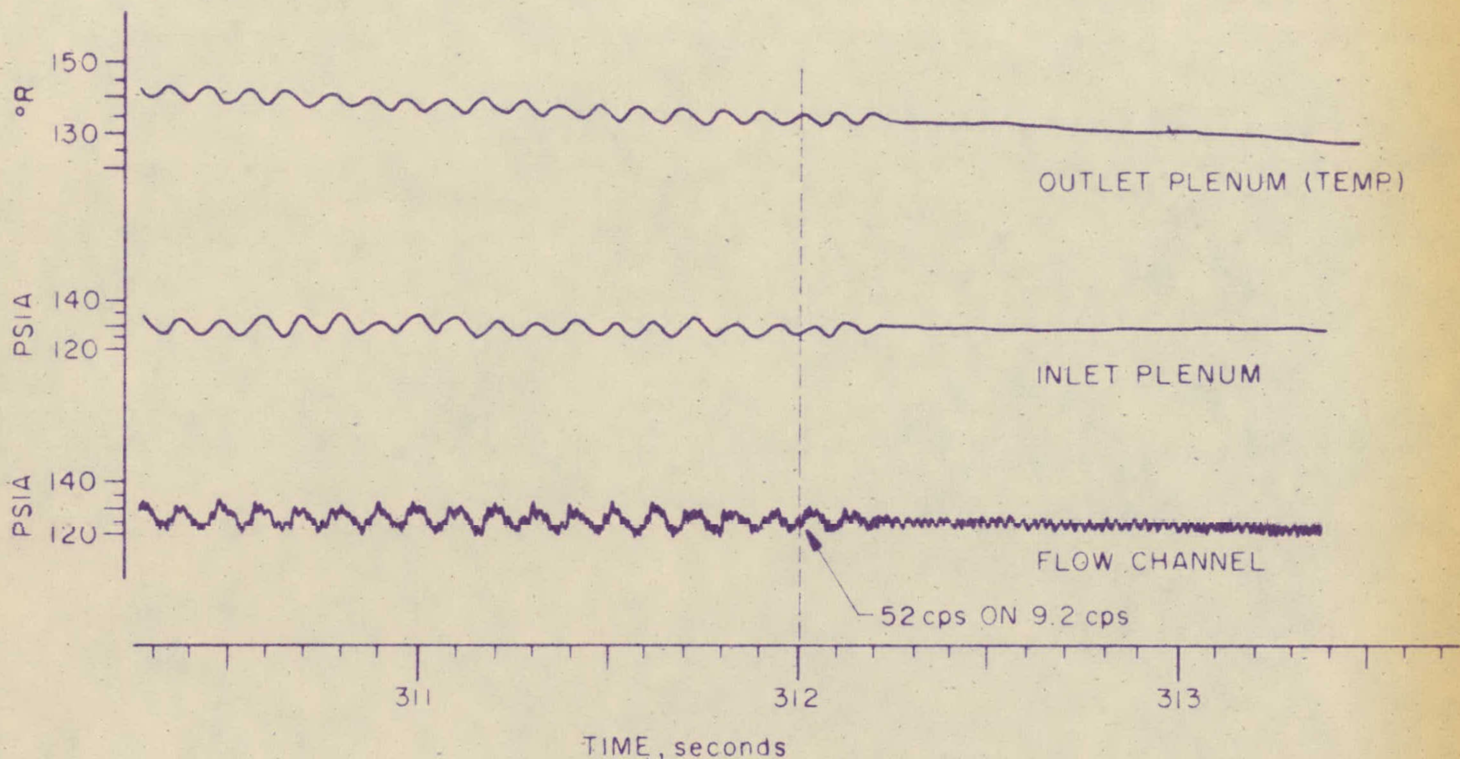

HYDROGEN EXPERIMENT OF OCTOBER 14, 1963

FIGURE 4

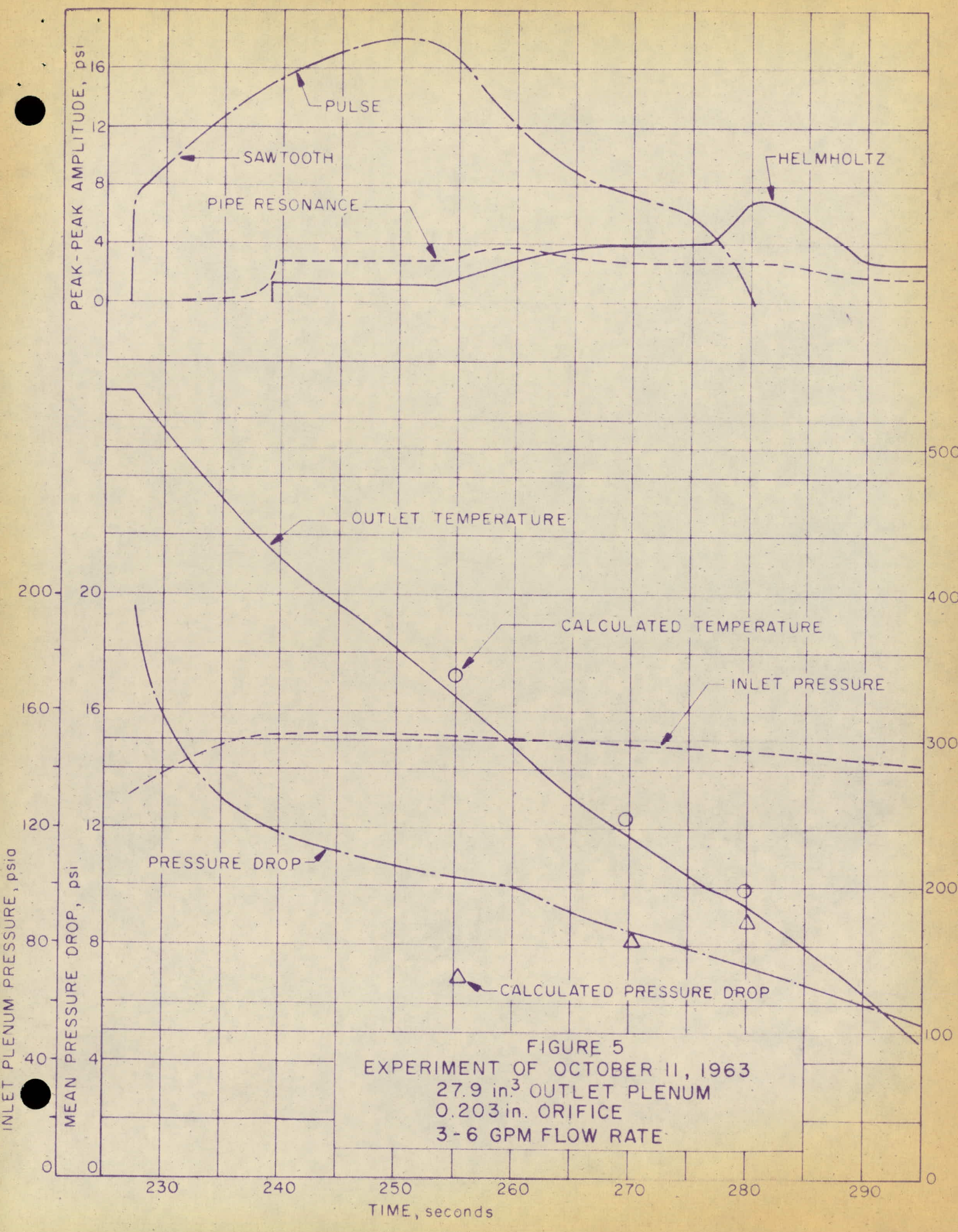

FIGURE 5
EXPERIMENT OF OCTOBER 11, 1963
27.9 in.^{3} OUTLET PLENUM
0.203 in. ORIFICE
3-6 GPM FLOW RATE

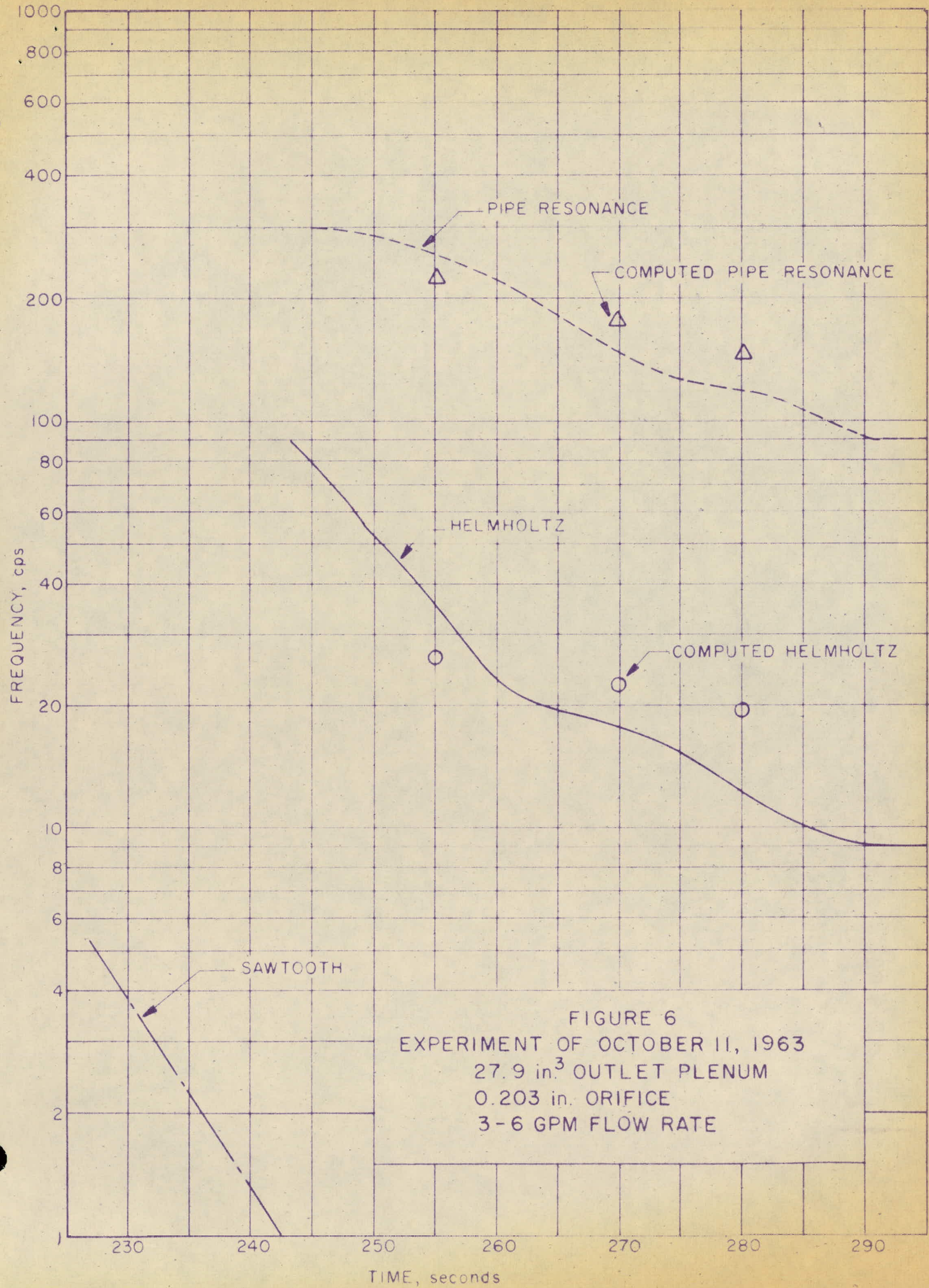

FIGURE 6
EXPERIMENT OF OCTOBER 11, 1963
27.9 $in.^3$ OUTLET PLENUM
0.203 in. ORIFICE
3-6 GPM FLOW RATE

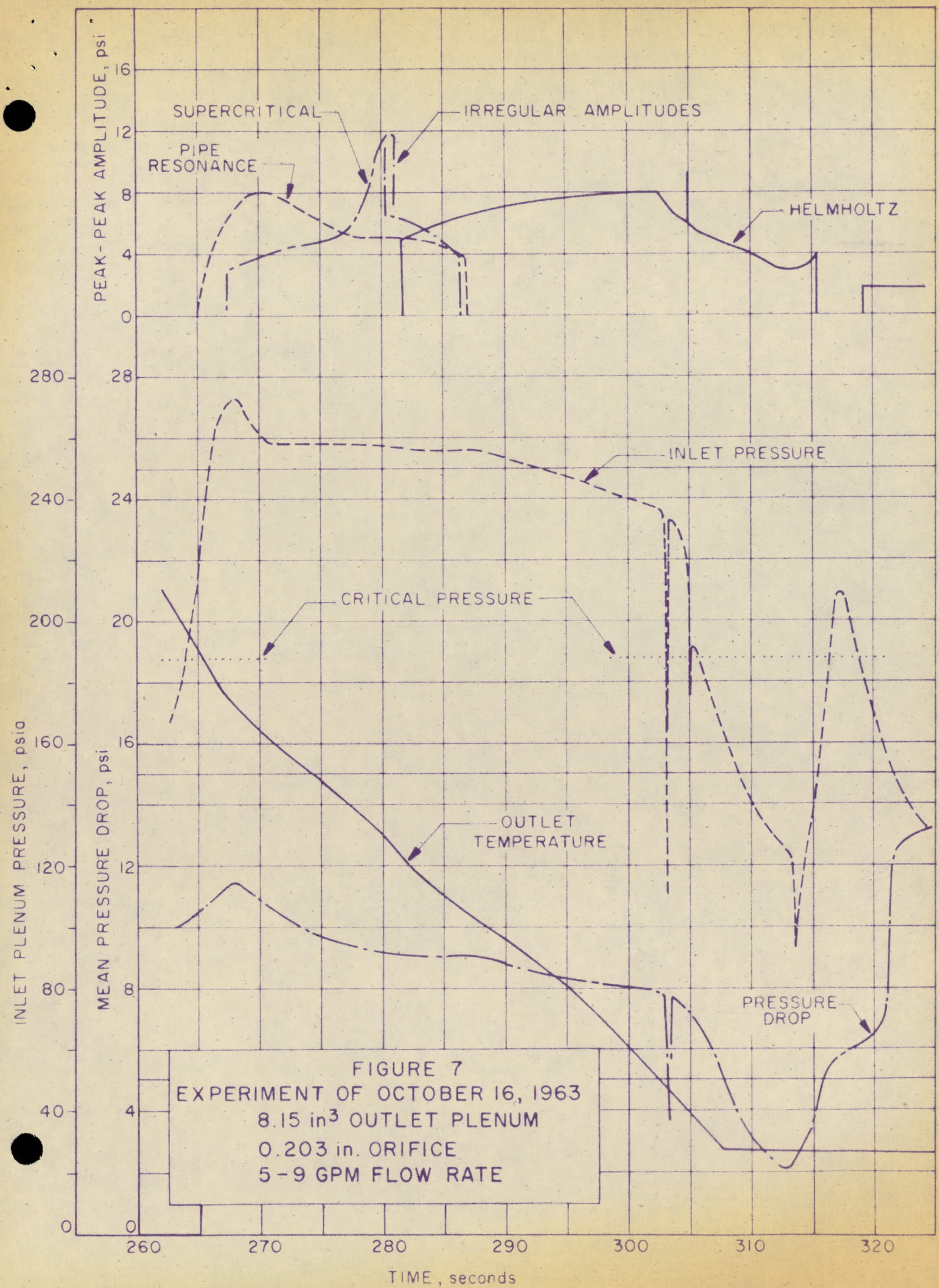

FIGURE 7
EXPERIMENT OF OCTOBER 16, 1963
8.15 in^3 OUTLET PLENUM
0.203 in. ORIFICE
5-9 GPM FLOW RATE

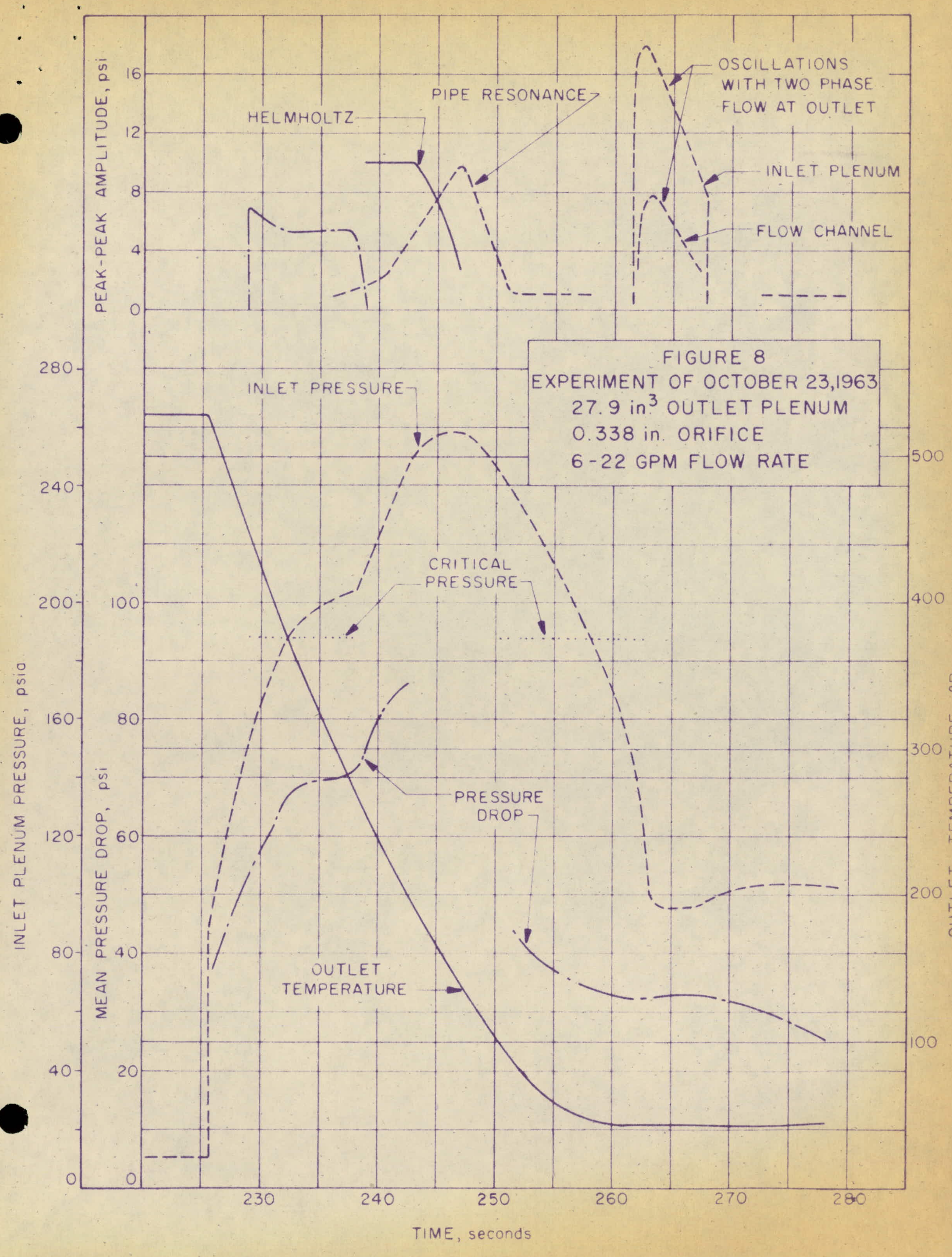

FIGURE 8
EXPERIMENT OF OCTOBER 23,1963
27.9 in^3 OUTLET PLENUM
0.338 in. ORIFICE
6-22 GPM FLOW RATE
PEAK-PEAK AMPLITUDE, psi
HELMHOLTZ
PIPE RESONANCE
OSCILLATIONS WITH TWO PHASE FLOW AT OUTLET
INLET PLENUM
FLOW CHANNEL
INLET PRESSURE
CRITICAL PRESSURE
PRESSURE DROP
OUTLET TEMPERATURE
INLET PLENUM PRESSURE, psia
MEAN PRESSURE DROP, psi
OUTLET TEMPERATURE, °R
TIME, seconds

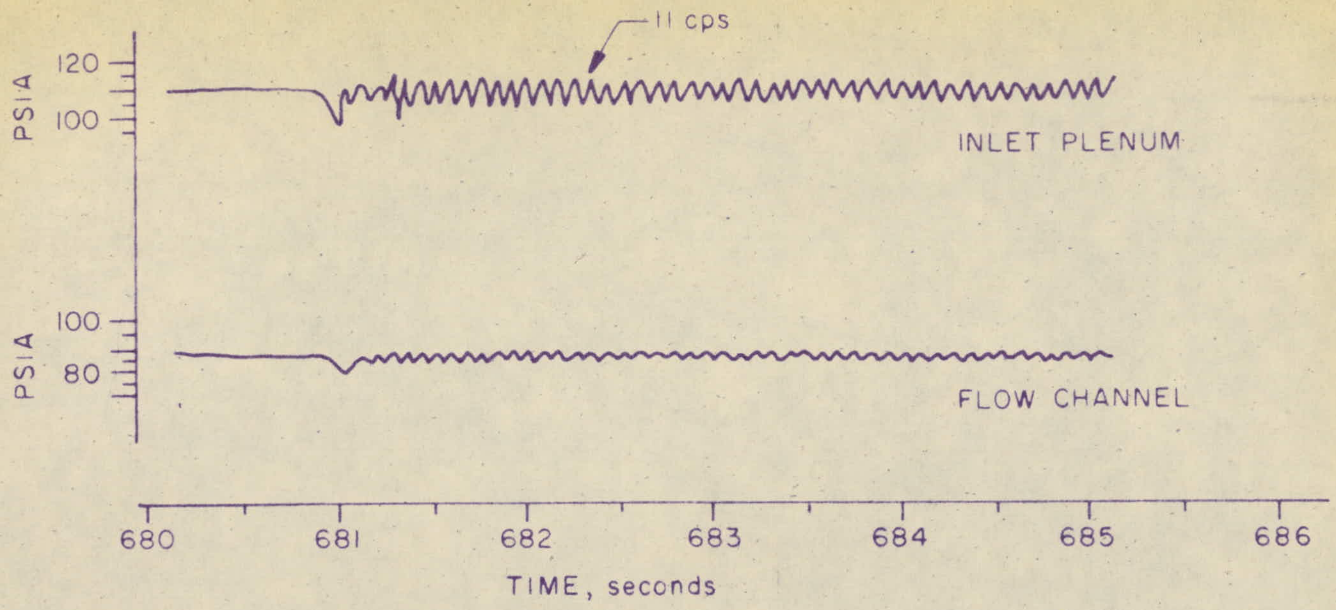

HYDROGEN EXPERIMENT OF NOVEMBER 6, 1963
SINGLE CHANNEL FLOW

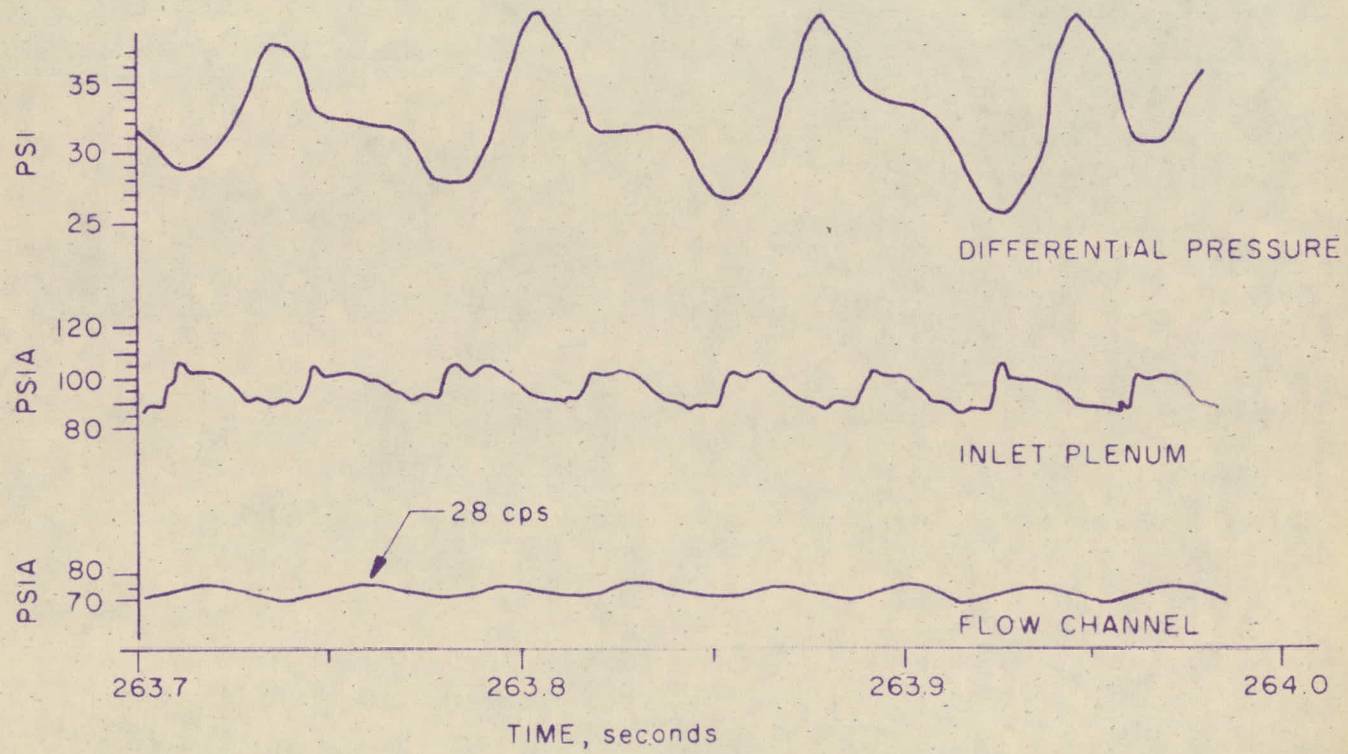

HYDROGEN EXPERIMENT OF OCTOBER 23, 1963
FOUR CHANNEL FLOW

FIGURE 9

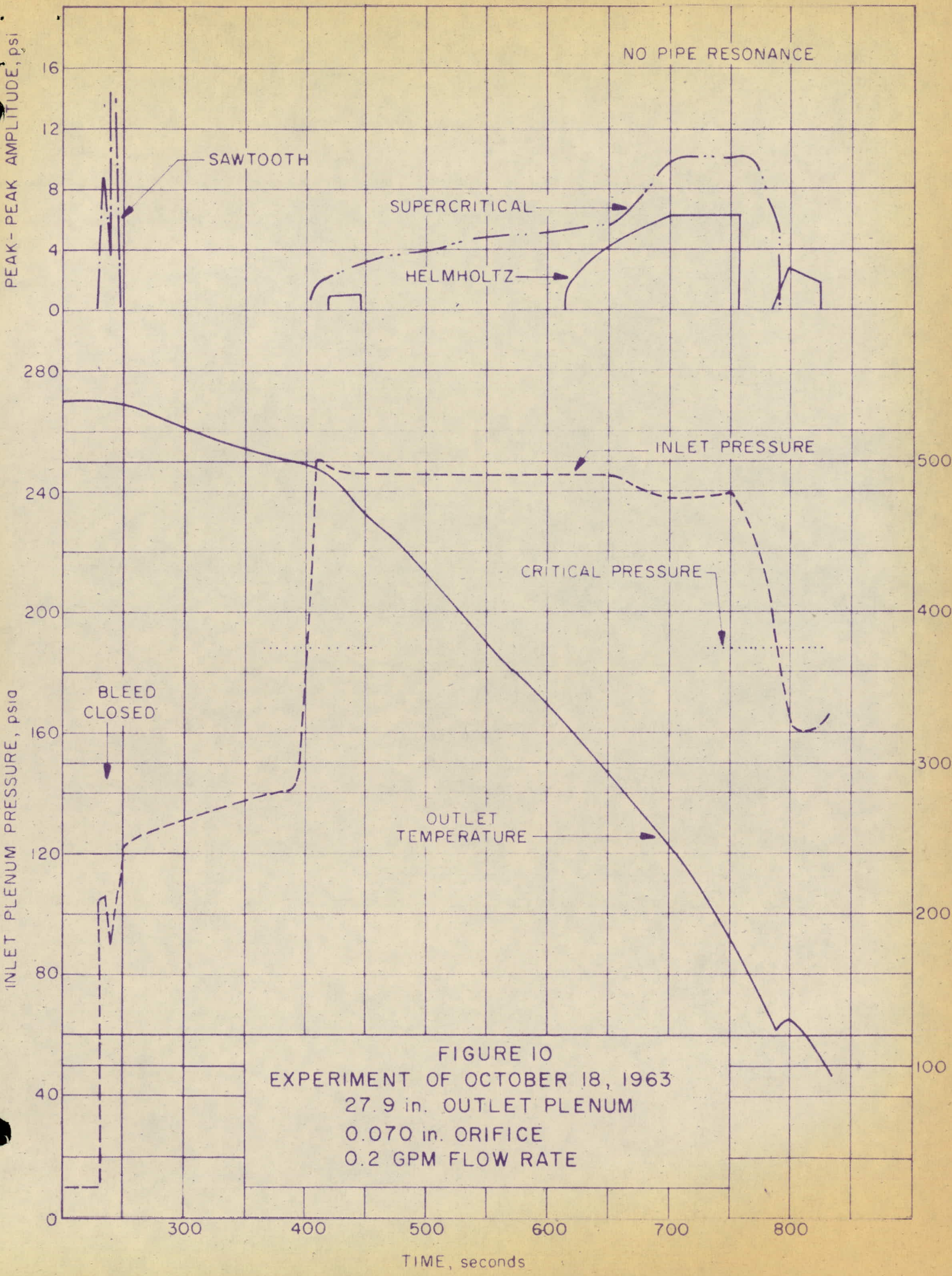

FIGURE 10
EXPERIMENT OF OCTOBER 18, 1963
27.9 in. OUTLET PLENUM
0.070 in. ORIFICE
0.2 GPM FLOW RATE

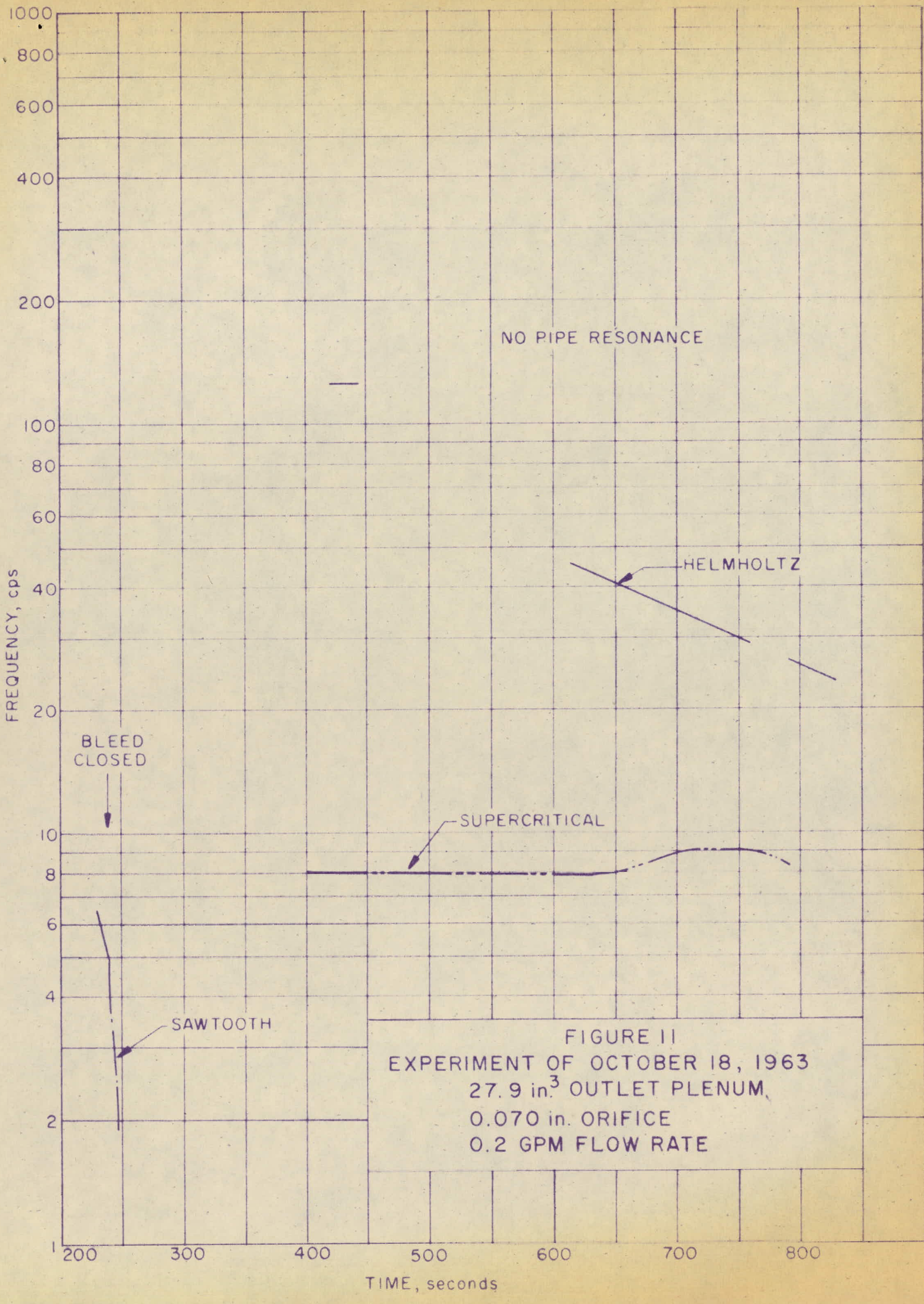

FIGURE 11
EXPERIMENT OF OCTOBER 18, 1963
27.9 in.^{3} OUTLET PLENUM,
0.070 in. ORIFICE
0.2 GPM FLOW RATE

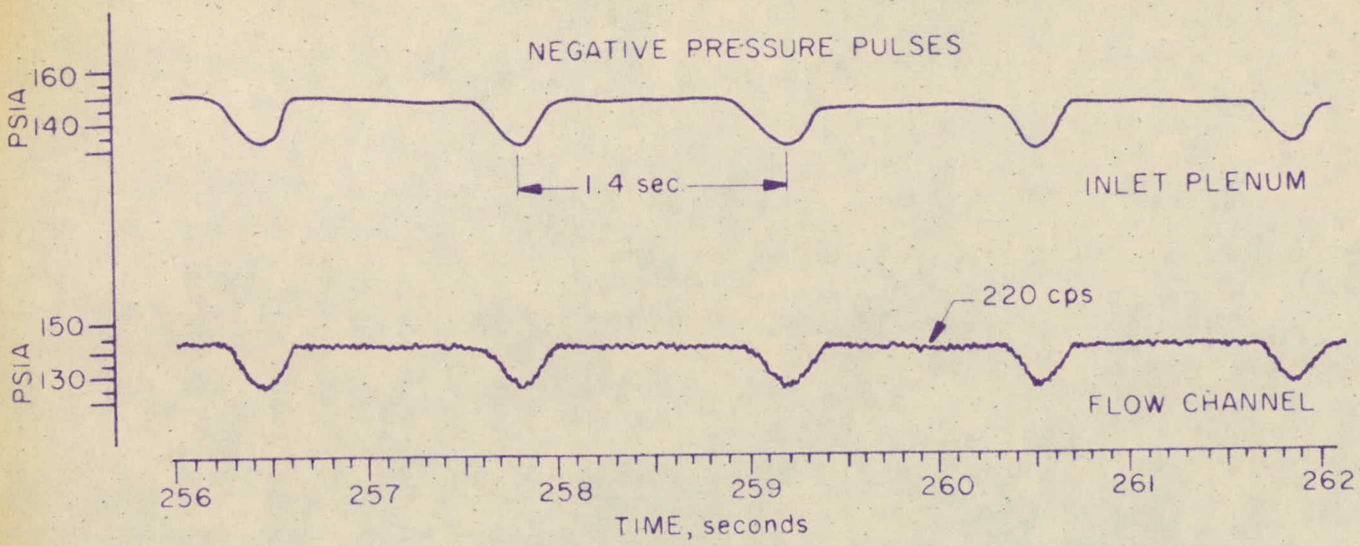

HYDROGEN EXPERIMENT OF OCTOBER 11, 1963

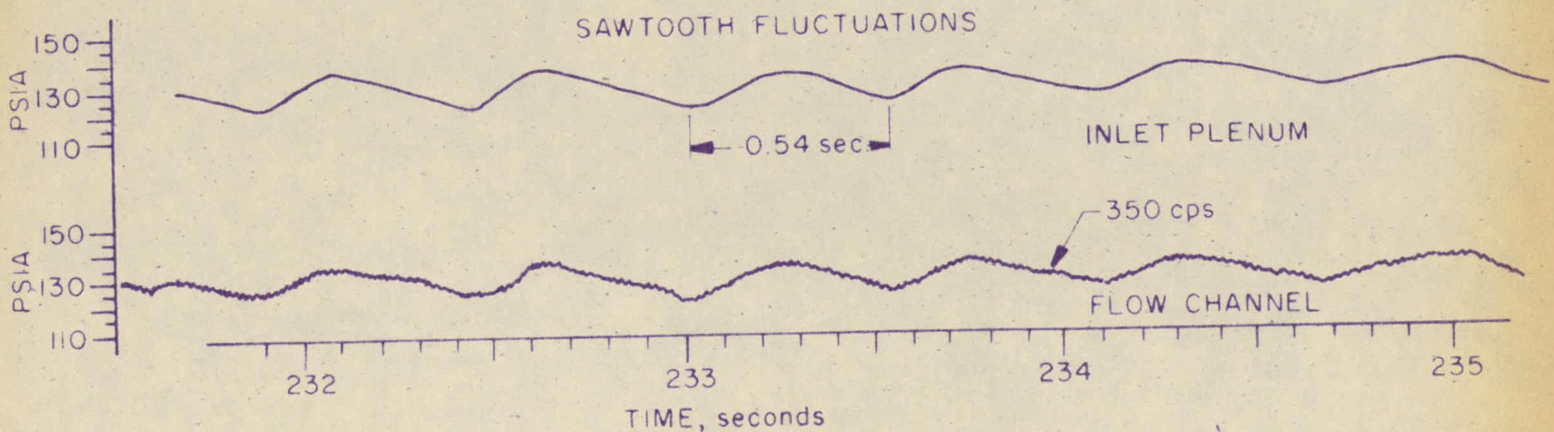

HYDROGEN EXPERIMENT OF OCTOBER 14, 1963

FIGURE 12

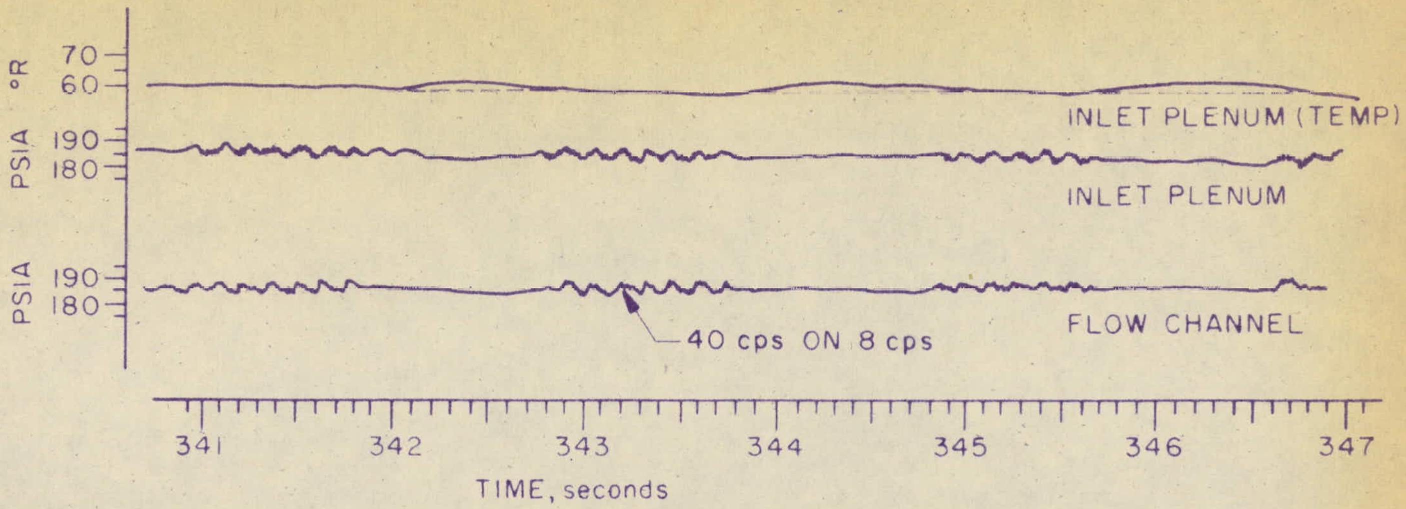

HYDROGEN EXPERIMENT OF OCTOBER 22, 1963

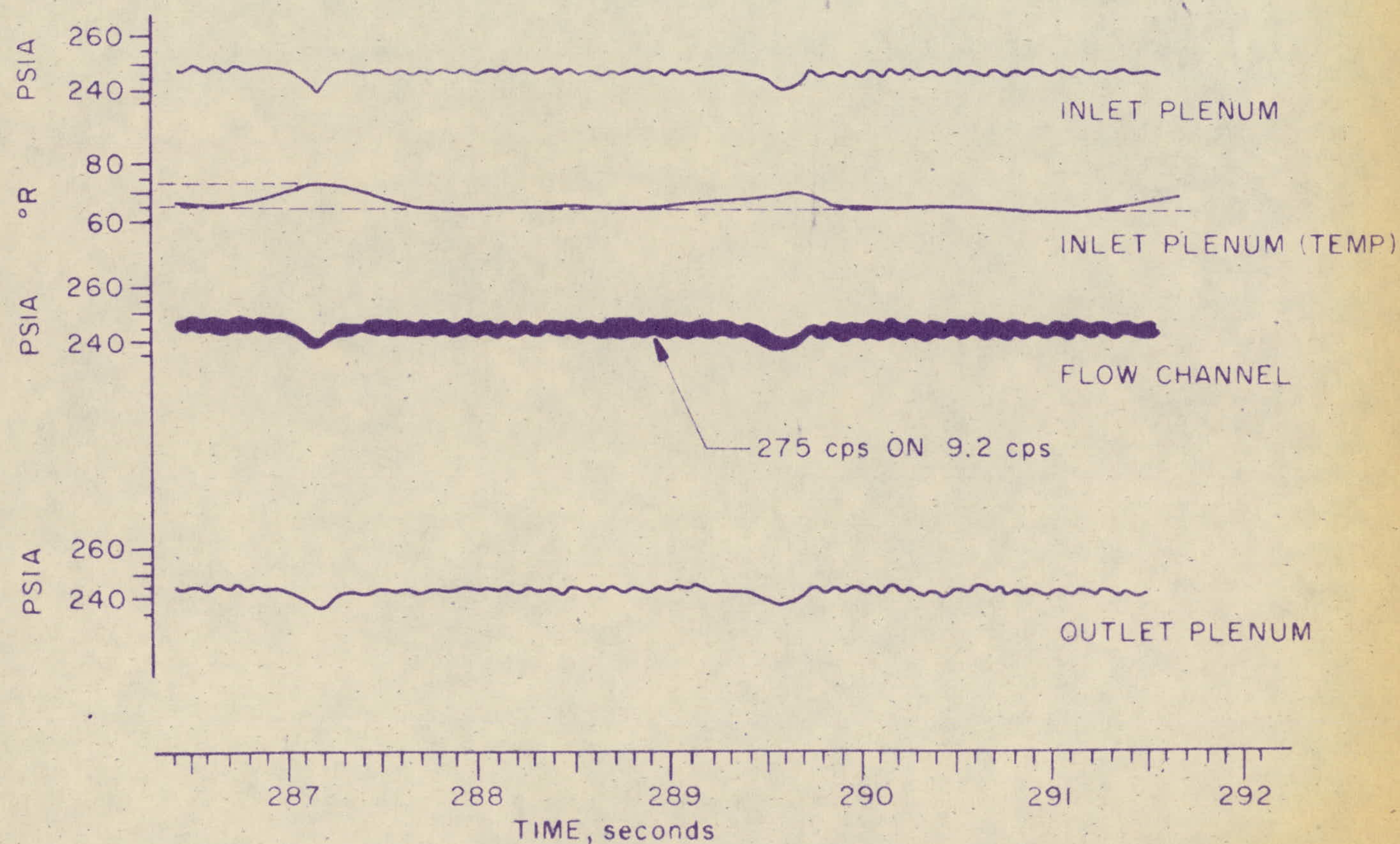

HYDROGEN EXPERIMENT OF OCTOBER 22, 1963

FIGURE 13

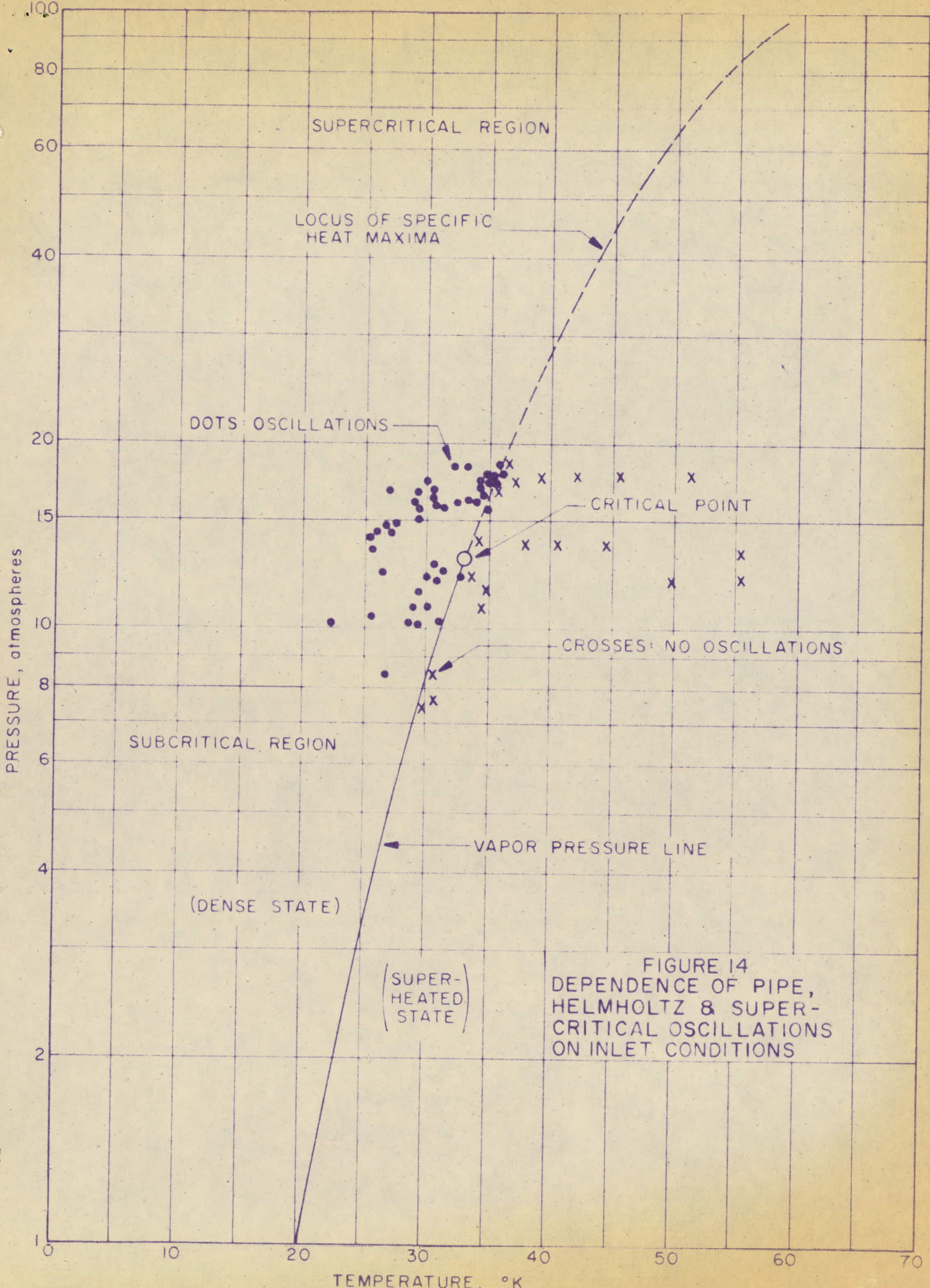

FIGURE 14
DEPENDENCE OF PIPE, HELMHOLTZ & SUPER-CRITICAL OSCILLATIONS ON INLET CONDITIONS